Available online at www.sciencedirect.com
ScienceDirect
Journal of Sound and Vibration 316 (2008) 101–121
JOURNAL OF SOUND AND VIBRATION
www.elsevier.com/locate/jsvi

Multiple augmentations of nonlinear systems and generalized minimum rank perturbations for damage detection ☆

Kiran D'Souza, Bogdan I. Epureanu*

Department of Mechanical Engineering, University of Michigan, 2350 Hayward Street, Ann Arbor, MI 48109-2125, USA

Received 3 August 2006; received in revised form 14 January 2008; accepted 14 February 2008
Handling Editor: P. Davies
Available online 2 April 2008

Abstract

A generalized minimum rank perturbation theory for identifying damage location and extent in nonlinear systems using a model-based approach is presented. This model updating method is able to handle changes in the mass, damping and stiffness parameters arising from the damage. The method uses a nonlinear discrete model of the system and the functional form of the nonlinearities to create an augmented linear model of the system. A modal analysis technique that uses forcing that is known but not prescribed is then used to solve for the modal properties of the augmented linear system after the onset of damage. The methodology has been demonstrated for cubic spring nonlinearities. In this work, the class of nonlinearities is expanded to include Coulomb friction. Several new algorithms are presented, including an iterative generalized minimum rank perturbation theory and a technique based on multiple augmentations to determine damages in linear and nonlinear parameters when there is an incomplete set of eigenvectors. Finally, two eigenvector filtering algorithms, which reduce the effects of measurement noise, are presented.

1. Introduction

Due to the increasing need for air and space technologies that are capable of operating in extreme environments for extended periods of time, there is a need for online damage detection and structural health monitoring techniques. Although there has been a great deal of research focused on structural health monitoring, most of the current methods ignore the effects of nonlinearities on the system dynamics, and use purely linear approaches. This is motivated in part by the fact that linear methods are more developed than nonlinear ones. Nonlinearities, however, are important in many structures and fluid-structural systems. Hence, methodologies that account for the effects of nonlinearities are needed.

Typically, damage detection methodologies use information about both the healthy and damaged systems. This information is in various forms, including a discrete or continuous model of the system, or modal properties of the (linearized) system. Most current methodologies then extract system features such as natural

☆ Earlier work on this approach has been presented at 2005 SDM and 2006 SPIE Conferences.

*Corresponding author.
E-mail address: epureanu@umich.edu (B.I. Epureanu).

0022-460X/$ - see front matter © 2008 Elsevier Ltd. All rights reserved.
doi:10.1016/j.jsv.2008.02.018

frequencies or mode shapes (for the linearized system) from measurements to detect damages. These (linear) features are obtained by using well established linear modal analysis techniques in either the time or frequency domain. These techniques are usually based on single input single output or multiple input multiple output approaches. A review of time-based multiple input multiple output approaches and their main characteristics was presented by Yang, Zhang, Li and Wu [1]. Such current available techniques include free and impulse response methods such as the poly-reference complex exponential [2], eigensystem realization algorithms [3] and Ibrahim time domain methods [4]. Also, forced response methods are available, such as auto-regressive moving average vector [5] and direct system parameter identification [6], which use the forcing from natural excitations to determine modal properties. The use of natural excitations makes these latter methods well-suited for online damage detection. Complementary to these linear methods, *nonlinear* experimental analyses are now under development. For example, nonlinear normal modes can be obtained by the harmonic balance method, invariant manifolds technique, method of multiple time scales, and asymptotic methods [7].

In a model-based approach, model parameters are identified first, and then used for structural health monitoring. Ibrahim and Saafan [8], and Heylen and Sas [9] provide a review of the four general categories of linear nondestructive evaluation. The first category is sensitivity methods, which use the modal sensitivity to parameter changes to identify damage. In this area, recently Leung et al. [10] proposed a more accurate solution technique for inverse sensitivity equations for asymmetric systems. The second is eigenstructure assignment techniques, which place eigenvalues and/or eigenvectors of the closed loop system. A good review of different eigenstructure assignment techniques can be found in the work by Andry et al. [11]. Lim [12] developed a constrained eigenstructure assignment for damage detection that formed a direct relation between the feedback control and structural parameter changes, while Jiang, Tang and Wang [13] developed optimal controllers for sensitivity enhancement by eigenstructure assignment. The third category includes optimal matrix update methods [14,15], which can be used for both system identification and damage detection. These methods update the system model using a set of constraints (e.g. maintaining the sparsity pattern of the original finite element model) for a given cost function (e.g. the minimum Frobenius norm for the update). The fourth and last category includes minimum rank perturbation methods [16–20], which solve for damage as the minimum rank solution to perturbation equations for the system. The key idea of minimum rank perturbation approaches is to exploit the fact that, for most physical models, there is a direct and simple relation between properties at one location in the system and the location of the corresponding entries of the matrices of the discrete system model. Hence, a localized damage corresponds to a localized change in system matrices. Thus, the change/perturbation of the system matrices is sparse and has low rank.

In this work, an algorithm that uses a system augmentation and a generalized minimum rank perturbation theory (GMRPT) [21,22] for nonlinear systems is developed and demonstrated to handle multiple simultaneous damages in linear and nonlinear parameters. The augmentation was shown to work for systems with cubic spring nonlinearities, and can be extended to any system where the functional form of the nonlinearity is known as a function of the state vector of the system and its derivatives. Control theory also uses a type of augmentation in the area of linear [23] and nonlinear [24,25] observers. However, the primary purpose of these observers is for state estimation coupled with state feedback to control the system. This differs significantly from the augmentation in this paper. The augmentation herein is used to generate an augmented (fictitious) linear system that follows a *single* trajectory of the real nonlinear system. This augmentation is not used to control the system, rather it is defined such that the augmented linear system follows (in a given subspace) a given trajectory of the nonlinear system while allowing for the use of linear theories for system identification and damage detection.

The augmentation requires that the forcing of the system be known but not prescribed. Hence, a technique such as direct system parameter identification [6] can be employed to perform the modal analysis (for the augmented system) to determine the modal properties of the augmented system since it uses as forcing the external excitations of the system. The augmented modal properties are then used by the generalized minimum rank perturbation theory [21], to determine damage location and extent. Generalized minimum rank perturbation theory was developed to handle the asymmetric damage scenarios that result from damage in the nonlinear portion of the system which, in turn, are due to the specialized nature of the augmentation.

A theoretical framework for the detection of simultaneous damages is developed herein, and several additions to the damage detection method proposed previously by the authors [21,22] are presented.

A subspace selection algorithm is used to reduce the effects of measurement noise. Also, an iterative approach to the solution of the left eigenvectors for simultaneous damage detection is employed. Moreover, an alternate approach is presented for the cases where an incomplete set of right eigenvectors are known. This new approach is based on multiple augmentations of the same nonlinear system. Finally, eigenvector filtering algorithms are discussed to reduce the effects of random measurement noise on damage detection. These techniques are demonstrated on nonlinear mass–spring systems and nonlinear frame structures. Complex simultaneous damage scenarios are explored and the effectiveness of the methodology for nonlinearities such as cubic springs and Coulomb friction are presented. Also, the influence of measurement noise with and without filtering algorithms is demonstrated through numerical simulations.

2. General methodology

In this section, the methodology for determining damage in nonlinear systems using system augmentation and generalized minimum rank perturbation theory [21] is presented. First, the augmentation procedure is described. Then, the procedure for detecting damage location and extent by generalized minimum rank perturbation theory is extended for the case of simultaneous damages in the mass, damping and stiffness parameters. Additionally, the damage detection methodology is extended by using multiple augmentations to determine damages in the nonlinear parameters in order to handle the cases where only an incomplete set of right eigenvectors are known. Finally, eigenvector filtering algorithms, which reduce the effects of noise, are detailed.

The work in this paper builds on three key papers which introduce and discuss minimum rank perturbation theory [16,19], generalized minimum rank perturbation theory, and system augmentation [21]. Although the following presentation of the methodology is self-contained, these three papers [16,19,21] provide additional detailed background on many of the approaches explicated herein.

2.1. System augmentation for modeling nonlinear systems

In this subsection, a method to model a single trajectory of a nonlinear system as a projection of the trajectory of an augmented linear system (of higher dimension) is presented. Consider a nonlinear system (characterized by a coordinate vector $\mathbf{x}$ and forced by an external excitation $\mathbf{g}(t)$) expressed as

$$\begin{bmatrix} \mathbf{M}_O & \mathbf{0} \\ \mathbf{0} & \mathbf{I} \end{bmatrix} \begin{bmatrix} \ddot{\mathbf{x}} \\ \dot{\mathbf{x}} \end{bmatrix} + \begin{bmatrix} \mathbf{D}_O & \mathbf{K}_O \\ -\mathbf{I} & \mathbf{0} \end{bmatrix} \begin{bmatrix} \dot{\mathbf{x}} \\ \mathbf{x} \end{bmatrix} + \begin{bmatrix} \mathbf{f}(\mathbf{x}, \dot{\mathbf{x}}, \ddot{\mathbf{x}}) \\ \mathbf{0} \end{bmatrix} = \begin{bmatrix} \mathbf{g}(t) \\ \mathbf{0} \end{bmatrix}, \tag{1}$$

where $\mathbf{M}_O$, $\mathbf{D}_O$, and $\mathbf{K}_O$ are the mass, damping, and stiffness matrices of the linearized system, and $\mathbf{f}$ is a nonlinear function. For a large category of nonlinearities, Eq. (1) can be rewritten as [21]

$$\mathbf{M}_O\ddot{\mathbf{x}} + \mathbf{D}_O\dot{\mathbf{x}} + \mathbf{K}_O\mathbf{x} + \mathbf{N}_I\ddot{\mathbf{y}} + \mathbf{N}_D\dot{\mathbf{y}} + \mathbf{N}_S\mathbf{y} = \mathbf{g}(t),$$

which in first-order matrix form becomes

$$\begin{bmatrix} \mathbf{M}_O & \mathbf{0} & \mathbf{N}_I & \mathbf{0} \\ \mathbf{0} & \mathbf{I} & \mathbf{0} & \mathbf{0} \\ \mathbf{0} & \mathbf{0} & \mathbf{N}_{AI} & \mathbf{0} \\ \mathbf{0} & \mathbf{0} & \mathbf{0} & \mathbf{I} \end{bmatrix} \begin{bmatrix} \ddot{\mathbf{x}} \\ \dot{\mathbf{x}} \\ \ddot{\mathbf{y}} \\ \dot{\mathbf{y}} \end{bmatrix} + \begin{bmatrix} \mathbf{D}_O & \mathbf{K}_O & \mathbf{N}_D & \mathbf{N}_S \\ -\mathbf{I} & \mathbf{0} & \mathbf{0} & \mathbf{0} \\ \mathbf{0} & \mathbf{N}_{CS} & \mathbf{N}_{AD} & \mathbf{N}_{AS} \\ \mathbf{0} & \mathbf{0} & -\mathbf{I} & \mathbf{0} \end{bmatrix} \begin{bmatrix} \dot{\mathbf{x}} \\ \mathbf{x} \\ \dot{\mathbf{y}} \\ \mathbf{y} \end{bmatrix} = \begin{bmatrix} \mathbf{g}(t) \\ \mathbf{0} \\ \mathbf{h}(t) \\ \mathbf{0} \end{bmatrix}, \tag{2}$$

where $\mathbf{N}_I$, $\mathbf{N}_{AI}$, $\mathbf{N}_D$, $\mathbf{N}_{AD}$, $\mathbf{N}_S$, $\mathbf{N}_{AS}$, and $\mathbf{N}_{CS}$ are constant matrices (more details are presented in the following), and $\mathbf{y}$ contains nonlinear terms. Eq. (2) may be written as a standard linear system as

$$\begin{bmatrix} \mathbf{M}_O & \mathbf{N}_I \\ \mathbf{0} & \mathbf{N}_{AI} \end{bmatrix} \begin{bmatrix} \ddot{\mathbf{x}} \\ \ddot{\mathbf{y}} \end{bmatrix} + \begin{bmatrix} \mathbf{D}_O & \mathbf{N}_D \\ \mathbf{0} & \mathbf{N}_{AD} \end{bmatrix} \begin{bmatrix} \dot{\mathbf{x}} \\ \dot{\mathbf{y}} \end{bmatrix} + \begin{bmatrix} \mathbf{K}_O & \mathbf{N}_S \\ \mathbf{N}_{CS} & \mathbf{N}_{AS} \end{bmatrix} \begin{bmatrix} \mathbf{x} \\ \mathbf{y} \end{bmatrix} = \begin{bmatrix} \mathbf{g}(t) \\ \mathbf{h}(t) \end{bmatrix},$$

$$\mathbf{M}\begin{bmatrix}\ddot{\mathbf{x}}\\ \ddot{\mathbf{y}}\end{bmatrix}+\mathbf{D}\begin{bmatrix}\dot{\mathbf{x}}\\ \dot{\mathbf{y}}\end{bmatrix}+\mathbf{K}\begin{bmatrix}\mathbf{x}\\ \mathbf{y}\end{bmatrix}=\begin{bmatrix}\mathbf{g}(t)\\ \mathbf{h}(t)\end{bmatrix}, \tag{3}$$

where **M**, **D**, and **K** are the mass, damping, and stiffness matrices of the augmented (linear) system. The function $\mathbf{h}(t)$ (in Eqs. (2) and (3)) is introduced to preserve most of the properties of the matrices in Eq. (1). The augmentation is expressed such that it matches the form of the nonlinearities in the systems of interest. One may note that the system can be augmented in several ways (by choosing $\mathbf{N}_{AI}$, $\mathbf{N}_{AD}$, $\mathbf{N}_{AS}$, and $\mathbf{N}_{CS}$) as to optimally suit various applications. Eq. (3) is the augmented linear model of the nonlinear system for which the eigenvalue problem must be solved.

2.1.1. Examples of augmentation

The specific form of the augmentation used is of crucial importance for the accuracy and robustness of the modal analysis technique used (e.g. direct system parameter identification). Hence, as discussed in the next subsection, the augmentation is done in a physical way [21]. Next, two examples of the augmentation for nonlinear one degree of freedom systems are presented. The first example illustrates how the augmentation is carried out for a cubic spring nonlinearity. The second example demonstrates how the augmentation is done for a Coulomb friction nonlinearity.

Consider an example of a one degree of freedom system with a mass connected to ground by a linear and a nonlinear (cubic) spring. The equation of motion of this simple nonlinear system can be written as

$$m\ddot{x}+kx+k_nx^3=g(t), \tag{4}$$

where m is the mass, k is the linear spring stiffness, and k_n is the nonlinear spring stiffness. Using a physically consistent augmentation developed by the authors [21] the new augmented system is represented by the following equation:

$$\begin{aligned} m\ddot{x}+kx+N_Sy&=g(t),\\ N_{AI}\ddot{y}+N_{AD}\dot{y}+N_{CS}x+N_{AS}y&=h(t). \end{aligned} \tag{5}$$

In this case, N_S and N_{CS} are both simply k_n, and y is x^3, while N_{AI}, N_{AD}, and N_{AS} are constants of our choosing. In this paper, N_{AI} was set to values of order of magnitude similar to the mass, N_{AS} was chosen to be multiples of k_n, and N_{AD} was set to zero. Finally, comparing Eqs. (2) and (4), one may note that N_I and N_D are zero.

The augmentation for Coulomb friction is distinct because Coulomb friction forces are discontinuous. The following is an example of how the augmentation is applied to a one degree of freedom mass connected to the ground by a linear spring and also rubbing against the ground. The equation of motion for this nonlinear system can be written as

$$m\ddot{x}+kx+\mu\,\mathrm{sign}(\dot{x})=g(t), \tag{6}$$

where μ is the coefficient of Coulomb friction. The augmentation described in this paper is represented by the following system:

$$\begin{aligned} m\ddot{x}+kx+N_I\ddot{y}&=g(t),\\ N_{AI}\ddot{y}+N_{AD}\dot{y}+N_{CS}x+N_{AS}y&=h(t). \end{aligned} \tag{7}$$

In this case, $\ddot{y}=\mathrm{sign}(\dot{x})$ and N_I is μ, while N_D and N_S are zero, and N_{AI}, N_{AD}, N_{CS} and N_{AS} are constants of our choosing. In this paper, μ was chosen for N_{AI}, zero was chosen for N_{AD}, and a constant was chosen for N_{AS}, while N_{CS} was simply set to the negative of N_{AS}.

2.1.2. Physical augmentation

Although there is a great amount of flexibility in choosing an augmentation for a system, most modal analysis techniques take advantage of certain physical properties of the systems they are identifying. In particular, most modal analysis techniques require the system matrices to be positive definite because these techniques are defined for vibration about a stable equilibrium. Next, an example of a brief proof of the

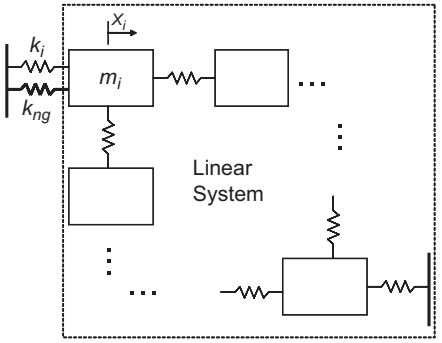

Fig. 1. Conceptual sketch of an n degree of freedom system with mass i connected to ground by a nonlinear spring.

positive definiteness of the augmented system matrices (such as the one in Eq. (5)) is given for a cubic spring connecting a mass to the ground. Consider an n degree of freedom system with a cubic spring connecting mass i to ground as shown in Fig. 1. The displacement of the system is given by $\mathbf{x}$, the nonlinear spring stiffness is k_{ng}, the augmented variable is $y = x_i^3$, and a is a parameter ($a \geqslant 0$) which characterizes the amount of damage in the nonlinear spring stiffness (e.g. $0 \leqslant a < 1$ for softening damage). The parameter b (which corresponds to the $\mathbf{N}_{CS}$) term equals one, while the parameter c (which corresponds to the $\mathbf{N}_{AS}$) term is greater than one. The mass matrix of the augmented system is diagonal with all positive entries, and is therefore positive definite. The augmented stiffness matrix is shown to be positive definite by showing that the following expression is positive for $\|\mathbf{x}\| + |y| \neq 0$, i.e.

$$[x_1 \ldots x_i \ldots x_n \;\; y] \begin{bmatrix} k_{1,1} & \ldots & k_{1,i} & \ldots & k_{1,n} & 0 \\ \vdots & \ddots & \vdots & & \vdots & \mathbf{0} \\ k_{i,1} & \ldots & k_{i,i} & \ldots & k_{i,n} & ak_{ng} \\ \vdots & & \vdots & \ddots & \vdots & \mathbf{0} \\ k_{n,1} & \ldots & k_{n,i} & \ldots & k_{n,n} & 0 \\ 0 & \mathbf{0} & bk_{ng} & \mathbf{0} & 0 & ck_{ng} \end{bmatrix} \begin{bmatrix} x_1 \\ \vdots \\ x_i \\ \vdots \\ x_n \\ y \end{bmatrix} = \Pi + (b+a)k_{ng}x_i y + ck_{ng}y^2 \geqslant 0. \tag{8}$$

Since $y^2 = x_i^6 \geqslant 0$, $x_i y = x_i^4 \geqslant 0$, and Π is the value from just the linear portion of the system, which is itself greater than zero, the only way the expression above can be equal to zero is when $\mathbf{x} = \mathbf{0}$ and $y = 0$. Similar proofs showing the positive definiteness can be obtained for a cubic spring connecting a mass to another mass and for the case of Coulomb friction, but they are omitted here for the sake of brevity.

2.1.3. Extraction of augmented modal properties

The extraction of modal properties from an augmented system requires a modal analysis technique which uses an excitation that is known, but not prescribed because the forcing term $\mathbf{h}(t)$ cannot be prescribed. Direct system parameter identification is a technique that resembles auto-regressive moving average vector and enables one to determine the mode shapes and natural frequencies of the system when the displacement of the degrees of freedom ($\mathbf{x}(t)$ and $\mathbf{y}(t)$) and the forcing ($\mathbf{g}(t)$ and $\mathbf{h}(t)$) are known. The requirement of the modal analysis technique to use a known but not prescribed forcing stems from the known but constrained forcing $\mathbf{h}(t)$. An example of implementation of the proposed approach is to measure the displacement vector $\mathbf{x}(t)$ and the forcing vector $\mathbf{g}(t)$. The vector $\mathbf{y}(t)$ is then computed from $\mathbf{x}(t)$, and the vector $\mathbf{h}(t)$ is calculated to satisfy Eq. (2).

A consequence of the manner in which the augmentation is done is the inability for damage to appear in the augmented parameters. This means that damage occurring in $\mathbf{N}_S$, $\mathbf{N}_D$ or $\mathbf{N}_I$ will only be reflected in the linear portion, and not the augmented portion of the system. The end result is that damage in nonlinear parameters causes asymmetrical changes in the system matrices when using augmentation.

2.2. Iterative generalized minimum rank perturbation theory for simultaneous damages

In this subsection, generalized minimum rank perturbation theory is extended to handle certain simultaneous damages in the mass, damping, and stiffness parameters. The work closely follows Kaouk, Zimmerman and Simmermacher with equations relating to the right eigenvectors developed in Ref. [16] and equations involving the left eigenvectors developed by the authors. First, the damage location algorithm is presented. Then, the damage extent algorithm for simultaneous damages is detailed. Finally, the iterative nature of the algorithm, caused by the approach employed for the calculation of the left eigenvectors, is presented.

2.2.1. Identification of damage location

To provide generalized minimum rank perturbation theory [21,22] with the degrees of freedom where damages are located, an algorithm which follows closely that of minimum rank perturbation theory [19] is used. In particular, it is assumed that a discrete, n-degree of freedom (e.g. finite element) model exists for the healthy augmented system, such that $\mathbf{M}$, $\mathbf{D}$, and $\mathbf{K}$ are the augmented $n \times n$ mass, (proportional) damping, and stiffness matrices. Hence, damage vectors $\mathbf{d}_i$ and $\mathbf{c}_i$ can be defined as

$$\begin{aligned} \mathbf{d}_i &\equiv \mathbf{Z}_{di}\mathbf{v}_{di} = (\lambda_{di}^2\Delta\mathbf{M} + \lambda_{di}\Delta\mathbf{D} + \Delta\mathbf{K})\mathbf{v}_{di}, \\ \mathbf{c}_i^{\mathrm{T}} &\equiv \mathbf{u}_{di}^{\mathrm{T}}\mathbf{Z}_{di} = \mathbf{u}_{di}^{\mathrm{T}}(\lambda_{di}^2\Delta\mathbf{M} + \lambda_{di}\Delta\mathbf{D} + \Delta\mathbf{K}), \quad \text{with} \\ \mathbf{Z}_{di} &\equiv \lambda_{di}^2\mathbf{M} + \lambda_{di}\mathbf{D} + \mathbf{K}, \end{aligned} \tag{9}$$

where the ith eigenvalue λ_{di}, ith right eigenvector $\mathbf{v}_{di}$, and ith left eigenvector $\mathbf{u}_{di}$ are of the damaged structure, and $\Delta\mathbf{M}$, $\Delta\mathbf{D}$ and $\Delta\mathbf{K}$ are the exact perturbation matrices (that reflect the nature of the structural damage).

A composite damage vector may be defined from (all or just a few) multiple measured modes as

$$\mathbf{d} = \frac{1}{q}\sum_{i=1}^{q}\frac{\mathbf{d}_i}{\|\mathbf{v}_{di}\|}, \tag{10}$$

where q is the number of measured modes.

Also, Zimmerman and Kaouk [19] developed an alternative view of the state of damage where Eq. (9) can be rewritten as

$$d_i^j \equiv \mathbf{z}_{di}^j\mathbf{v}_{di} = \|\mathbf{z}_{di}^j\|\|\mathbf{v}_{di}\|\cos(\theta_i^j), \tag{11}$$

where d_i^j is the jth component (i.e. jth degree of freedom) of the ith damage vector, $\mathbf{z}_{di}^j$ is the jth row of the matrix $\mathbf{Z}_{di}$, and θ_i^j is the angle between the vectors $\mathbf{z}_{di}^j$ and $\mathbf{v}_{di}$. A damage detector α_i^j may be calculated from θ_i^j as

$$\alpha_i^j = \theta_i^j\left(\frac{180^\circ}{\pi}\right) - 90^\circ. \tag{12}$$

Finally, a composite damage vector $\boldsymbol{\gamma}$ may be defined from the multiple measured modes as

$$\boldsymbol{\gamma}_j = \frac{1}{q}\sum_{i=1}^{q}|\boldsymbol{\alpha}_i^j|. \tag{13}$$

The indexes j where d_i^j, α_i^j or γ_j are large are the identified locations of damage. We denote by p the number of such locations.

2.2.2. Damage isolation

Once the damage location is known, the next step in assessing structural health is to determine the damage extent by isolating which system matrices are affected by damage. Following closely the work developed in minimum rank perturbation theory [16], we extended the previous approach for the case of asymmetric damage scenarios. This section uses the cross-orthogonality properties of the modes to the system matrices

and a specialized pseudo-inverse developed in Ref. [16]. Using the information garnered from the damage location algorithm, damage location matrices, **B** and **A** can be defined as

$$\begin{aligned}\mathbf{M}\mathbf{V}_d\boldsymbol{\Lambda}_d^2+\mathbf{D}\mathbf{V}_d\boldsymbol{\Lambda}_d+\mathbf{K}\mathbf{V}_d=\Delta\mathbf{M}\mathbf{V}_d\boldsymbol{\Lambda}_d^2+\Delta\mathbf{D}\mathbf{V}_d\boldsymbol{\Lambda}_d+\Delta\mathbf{K}\mathbf{V}_d\equiv\mathbf{B},\\ \boldsymbol{\Lambda}_d^2\mathbf{U}_d^{\mathrm{T}}\mathbf{M}+\boldsymbol{\Lambda}_d\mathbf{U}_d^{\mathrm{T}}\mathbf{D}+\mathbf{U}_d^{\mathrm{T}}\mathbf{K}=\boldsymbol{\Lambda}_d^2\mathbf{U}_d^{\mathrm{T}}\Delta\mathbf{M}+\boldsymbol{\Lambda}_d\mathbf{U}_d^{\mathrm{T}}\Delta\mathbf{D}+\mathbf{U}_d^{\mathrm{T}}\Delta\mathbf{K}\equiv\mathbf{A}^{\mathrm{T}},\end{aligned}\tag{14}$$

where

$$\boldsymbol{\Lambda}_d=\mathrm{diag}(\lambda_{d1},\lambda_{d2}\ldots\lambda_{dq}),$$

$$\mathbf{V}_d=[\mathbf{v}_{d1},\mathbf{v}_{d2}\ldots\mathbf{v}_{dq}],$$

$$\mathbf{B}=[\mathbf{d}_1,\mathbf{d}_2\ldots\mathbf{d}_q],$$

$$\mathbf{U}_d^{\mathrm{T}}=[\mathbf{u}_{d1},\mathbf{u}_{d2}\ldots\mathbf{u}_{dq}]^{\mathrm{T}},$$

$$\mathbf{A}^{\mathrm{T}}=[\mathbf{c}_1,\mathbf{c}_2\ldots\mathbf{c}_q]^{\mathrm{T}}.$$

Note that **B** and **A** can be determined from the original system matrices (**M**, **D**, **K**) and only p of the measured damaged eigenvalues and eigenvectors. However, using the subspace selection algorithm for GMRPT (presented below), all q measured modes ($q>p$) can be used to define **B** and **A** to obtain more accurate results.

Matrices **B** and **A** contain contributions of force imbalances due to the damage in the mass, damping and stiffness parameters. The matrix **B** is precisely that used by Kaouk et al. [16]. This force imbalance can be written as

$$\mathbf{B}=\mathbf{B}_M\boldsymbol{\Lambda}_d^2+\mathbf{B}_D\boldsymbol{\Lambda}_d+\mathbf{B}_K,\tag{15}$$

where

$$\mathbf{B}_M=\Delta\mathbf{M}\mathbf{V}_d,\quad \mathbf{B}_D=\Delta\mathbf{D}\mathbf{V}_d,\quad \mathbf{B}_K=\Delta\mathbf{K}\mathbf{V}_d,\tag{16}$$

and

$$\mathbf{A}=\mathbf{A}_M\boldsymbol{\Lambda}_d^2+\mathbf{A}_D\boldsymbol{\Lambda}_d+\mathbf{A}_K,\tag{17}$$

where

$$\mathbf{A}_M=\Delta\mathbf{M}^{\mathrm{T}}\mathbf{U}_d,\quad \mathbf{A}_D=\Delta\mathbf{D}^{\mathrm{T}}\mathbf{U}_d,\quad \mathbf{A}_K=\Delta\mathbf{K}^{\mathrm{T}}\mathbf{U}_d.\tag{18}$$

The motivation for expressing **B** and **A** as in Eqs. (15) and (17), is that force imbalances due to the mass, damping, and stiffness matrices are separated according to their respective matrix. The matrices $\mathbf{B}_M$, $\mathbf{B}_D$, $\mathbf{B}_K$, $\mathbf{A}_M$, $\mathbf{A}_D$ and $\mathbf{A}_K$ can be determined using the cross-orthogonality relations that arise from the proportional damping assumption. By extracting mass normalized right and left eigenvectors, the cross-orthogonality relations of the damaged system can be expressed as

$$\begin{aligned}\mathbf{U}_d^{\mathrm{T}}(\mathbf{M}-\Delta\mathbf{M})\mathbf{V}_d&=\mathbf{I}_{q\times q},\\ \mathbf{U}_d^{\mathrm{T}}(\mathbf{D}-\Delta\mathbf{D})\mathbf{V}_d&=\mathrm{diag}(2\zeta_{d1}\lambda_{d1}\ldots2\zeta_{dq}\lambda_{dq})=\boldsymbol{\Sigma}_d,\\ \mathbf{U}_d^{\mathrm{T}}(\mathbf{K}-\Delta\mathbf{K})\mathbf{V}_d&=\mathrm{diag}(\lambda_{d1}^2\ldots\lambda_{dq}^2)=\boldsymbol{\Lambda}_d^2,\end{aligned}\tag{19}$$

where ζ_{di} is the damping ratio for the ith mode of the damaged structure. Rearranging Eq. (19) yields

$$\begin{aligned}\mathbf{U}_d^{\mathrm{T}}\Delta\mathbf{M}\mathbf{V}_d&=\mathbf{U}_d^{\mathrm{T}}\mathbf{M}\mathbf{V}_d-\mathbf{I}_{q\times q}\equiv\mathbf{U}_d^{\mathrm{T}}\mathbf{B}_M,\\ \mathbf{U}_d^{\mathrm{T}}\Delta\mathbf{D}\mathbf{V}_d&=\mathbf{U}_d^{\mathrm{T}}\mathbf{D}\mathbf{V}_d-\boldsymbol{\Sigma}_d\equiv\mathbf{U}_d^{\mathrm{T}}\mathbf{B}_D,\\ \mathbf{U}_d^{\mathrm{T}}\Delta\mathbf{K}\mathbf{V}_d&=\mathbf{U}_d^{\mathrm{T}}\mathbf{K}\mathbf{V}_d-\boldsymbol{\Lambda}_d^2\equiv\mathbf{U}_d^{\mathrm{T}}\mathbf{B}_K.\end{aligned}\tag{20}$$

Similarly, Eq. (19) can be rearranged to yield relations for the force imbalances in the **A** matrices to obtain

$$\begin{aligned}\mathbf{V}_d^{\mathrm{T}}\mathbf{A}_M &\equiv \mathbf{V}_d^{\mathrm{T}}\mathbf{M}^{\mathrm{T}}\mathbf{U}_d - \mathbf{I}_{q\times q},\\ \mathbf{V}_d^{\mathrm{T}}\mathbf{A}_D &\equiv \mathbf{V}_d^{\mathrm{T}}\mathbf{D}^{\mathrm{T}}\mathbf{U}_d - \mathbf{\Sigma}_d,\\ \mathbf{V}_d^{\mathrm{T}}\mathbf{A}_K &\equiv \mathbf{V}_d^{\mathrm{T}}\mathbf{K}^{\mathrm{T}}\mathbf{U}_d - \mathbf{\Lambda}_d^2.\end{aligned} \tag{21}$$

All the damage location matrices, $\mathbf{B}_M$, $\mathbf{B}_D$, $\mathbf{B}_K$, $\mathbf{A}_M$, $\mathbf{A}_D$ and $\mathbf{A}_K$, can be calculated from Eqs. (20) and (21). In the case where the number of measured modes equals the number of degrees of freedom in the model (i.e. $q = n$), these matrices can be computed by using the inverses of $\mathbf{V}_d$ and $\mathbf{U}_d$. However, often the number of measured modes is much less than the size of the model ($q \ll n$). For this case, the use of the Moore–Penrose pseudo-inverse of the matrices $\mathbf{V}_d$ and $\mathbf{U}_d$ comes to mind. Unfortunately, the sparsity of **B** and **A** would not be reflected in $\mathbf{B}_M$, $\mathbf{B}_D$, $\mathbf{B}_K$, $\mathbf{A}_M$, $\mathbf{A}_D$ and $\mathbf{A}_K$. Hence, the minimality of the rank of the variation in the mass, damping and stiffness matrices cannot be capitalized upon. Nonetheless, this problem can be overcome by defining a pseudo-inverse that preserves the sparsity of the damage location matrices **B** and **A**. For matrix **B**, this has been proposed by Kaouk et al. [16]. This approach results in solving for the $n \times q$ real matrices $\mathbf{P}_B$ and $\mathbf{P}_A$ as follows:

$$\begin{aligned}&\mathbf{P}_B(\mathbf{U}_d^{\mathrm{T}}\mathbf{B}) = \mathbf{B},\\ &\mathbf{P}_A(\mathbf{V}_d^{\mathrm{T}}\mathbf{A}) = \mathbf{A},\end{aligned} \quad \text{so that} \quad \begin{aligned}&\mathbf{P}_B = \mathbf{B}(\mathbf{U}_d^{\mathrm{T}}\mathbf{B})^{-1},\\ &\mathbf{P}_A = \mathbf{A}(\mathbf{V}_d^{\mathrm{T}}\mathbf{A})^{-1}.\end{aligned} \tag{22}$$

Once $\mathbf{P}_B$ and $\mathbf{P}_A$ are computed, $\mathbf{B}_M$, $\mathbf{B}_D$, $\mathbf{B}_K$, $\mathbf{A}_M$, $\mathbf{A}_D$, and $\mathbf{A}_K$ can be calculated using Eqs. (20) and (21) as

$$\begin{aligned}\mathbf{B}_M &= \mathbf{P}_B(\mathbf{U}_d^{\mathrm{T}}\mathbf{M}\mathbf{V}_d - \mathbf{I}_{q\times q}),\\ \mathbf{B}_D &= \mathbf{P}_B(\mathbf{U}_d^{\mathrm{T}}\mathbf{D}\mathbf{V}_d - \mathbf{\Sigma}_d),\\ \mathbf{B}_K &= \mathbf{P}_B(\mathbf{U}_d^{\mathrm{T}}\mathbf{K}\mathbf{V}_d - \mathbf{\Lambda}_d^2),\end{aligned} \quad \text{and} \quad \begin{aligned}\mathbf{A}_M &= \mathbf{P}_A(\mathbf{V}_d^{\mathrm{T}}\mathbf{M}^{\mathrm{T}}\mathbf{U}_d - \mathbf{I}_{q\times q}),\\ \mathbf{A}_D &= \mathbf{P}_A(\mathbf{V}_d^{\mathrm{T}}\mathbf{D}^{\mathrm{T}}\mathbf{U}_d - \mathbf{\Sigma}_d),\\ \mathbf{A}_K &= \mathbf{P}_A(\mathbf{V}_d^{\mathrm{T}}\mathbf{K}^{\mathrm{T}}\mathbf{U}_d - \mathbf{\Lambda}_d^2).\end{aligned} \tag{23}$$

From Eq. (22) it is clear that $\mathbf{P}_B$ and $\mathbf{P}_A$ have the same sparsity pattern as matrices **B** and **A**, respectively. Therefore, matrices $\mathbf{B}_M$, $\mathbf{B}_D$, $\mathbf{B}_K$ will also reflect the sparsity pattern of **B**, while $\mathbf{A}_M$, $\mathbf{A}_D$ and $\mathbf{A}_K$ will reflect the sparsity pattern of **A**.

2.2.3. Equations of generalized minimum rank perturbation theory

In this section, the equations of generalized minimum rank perturbation theory are only outlined. For a more complete proof the reader is referred to Ref. [21]. The work presented in Ref. [21] discusses minimal rank solutions for asymmetric damage cases, and is a generalization of symmetric damage cases developed in Ref. [19]. This section provides the unique solution to the unknown perturbation matrices from Eqs. (24) and (25) that is minimum rank. For clarity, the following discussion is for the case where $q = p$. Nonetheless, the generalized minimum rank perturbation theory subspace selection algorithm directly extends these results for the case where $q > p$. The only unknowns in Eqs. (16) and (18) are the damage perturbation matrices. Each of the three equations in Eq. (16) can be expressed as

$$\mathbf{C}\mathbf{X}_B = \mathbf{Y}_B, \tag{24}$$

where matrices $\mathbf{X}_B$ and $\mathbf{Y}_B$ are known (e.g. $\mathbf{X}_B = \mathbf{V}_d$ and $\mathbf{Y}_B = \mathbf{B}_M$), and matrix **C** is unknown (e.g. $\mathbf{C} = \Delta\mathbf{M}$). Also, each of the three equations in Eq. (18) can be expressed as

$$\mathbf{C}^{\mathrm{T}}\mathbf{X}_A = \mathbf{Y}_A, \tag{25}$$

where matrices $\mathbf{X}_A$ and $\mathbf{Y}_A$ are known (e.g. $\mathbf{X}_A = \mathbf{U}_d$ and $\mathbf{Y}_A = \mathbf{A}_M$). The minimum rank solution **C** of Eqs. (24) and (25) is unique and can be expressed as

$$\mathbf{C} = \mathbf{Y}_B\mathbf{H}\mathbf{Y}_A^{\mathrm{T}}, \quad \text{with} \quad \mathbf{H} = (\mathbf{Y}_A^{\mathrm{T}}\mathbf{X}_B)^{-1}. \tag{26}$$

This solution given by generalized minimum rank perturbation theory [21] is unique and of rank p, where $\mathbf{X}_B$, $\mathbf{X}_A$, $\mathbf{Y}_B$, and $\mathbf{Y}_A \in \Re^{n\times p}$ are given, with $p<n$ and $\text{rank}(\mathbf{C}) = \text{rank}(\mathbf{X}_B) = \text{rank}(\mathbf{X}_A) = \text{rank}(\mathbf{Y}_B) = \text{rank}(\mathbf{Y}_A) = p$.

2.2.4. Generalized minimum rank perturbation theory subspace selection

Experimental modal data is always affected by measurement and eigenvector/eigenvalue extraction noise. In this section, a subspace selection algorithm, which reduces the influence of noise, is presented. This algorithm is the same as the one developed by Kaouk et al. [16] for MRPT, but it has been extended for GMRPT. This section uses a singular value decomposition of the force imbalance matrices (e.g. $\mathbf{B}_m$) to filter out noise. The subspace selection algorithm is defined as the numerically well conditioned search for two matrices $\mathbf{Z}_B \in \Re^{q\times\hat{p}_B}$ and $\mathbf{Z}_A \in \Re^{q\times\hat{p}_A}$ such that

$$\mathbf{C}\mathbf{X}_B\mathbf{Z}_B = \mathbf{Y}_B\mathbf{Z}_B, \quad \text{and} \quad \mathbf{C}^{\mathrm{T}}\mathbf{X}_A\mathbf{Z}_A = \mathbf{Y}_A\mathbf{Z}_A. \tag{27}$$

The unknowns are $\hat{p}_B$ and $\hat{p}_A$, i.e. the numerical rank of $\mathbf{Y}_B$, $\mathbf{Y}_A$, and $\mathbf{Z}_B$, $\mathbf{Z}_A$. Note that $\hat{p}_B<q$ and $\hat{p}_A<q$. Consider the singular value decomposition of $\mathbf{Y}_B$ and $\mathbf{Y}_A$ defined as

$$\begin{aligned}\mathbf{Y}_B &= [\mathbf{U}_{B1}\ \ \mathbf{U}_{B2}]\begin{bmatrix}\mathbf{\Sigma}_B & \mathbf{0}\\ \mathbf{0} & \mathbf{\Sigma}_{\varepsilon B}\end{bmatrix}[\mathbf{V}_{B1}\ \ \mathbf{V}_{B2}]^{\mathrm{T}},\\ \mathbf{Y}_A &= [\mathbf{U}_{A1}\ \ \mathbf{U}_{A2}]\begin{bmatrix}\mathbf{\Sigma}_A & \mathbf{0}\\ \mathbf{0} & \mathbf{\Sigma}_{\varepsilon A}\end{bmatrix}[\mathbf{V}_{A1}\ \ \mathbf{V}_{A2}]^{\mathrm{T}},\end{aligned} \tag{28}$$

where $\mathbf{\Sigma}_B$ and $\mathbf{\Sigma}_A$ include singular values larger than ε, while $\mathbf{\Sigma}_{\varepsilon B}$ and $\mathbf{\Sigma}_{\varepsilon A}$ include singular values smaller than ε (where ε is a small positive constant which approximates zero). Also, $\mathbf{U}_B$, $\mathbf{V}_B$ and $\mathbf{U}_A$, $\mathbf{V}_A$ are the left and right singular vectors in partitioned form for $\mathbf{Y}_B$ and $\mathbf{Y}_A$. When $\mathbf{Y}_B$ is rank deficient, the range of $\mathbf{Y}_B$ is spanned by the $\hat{p}_B$ columns of $\mathbf{U}_{B1}$. Therefore, the goal is to find matrices $\mathbf{Z}_B$ and $\mathbf{Z}_A$ such that

$$\mathbf{Y}_B\mathbf{Z}_B = \mathbf{U}_{B1}, \quad \text{and} \quad \mathbf{Y}_A\mathbf{Z}_A = \mathbf{U}_{A1}. \tag{29}$$

The matrices $\mathbf{Z}_B$ and $\mathbf{Z}_A$ can be calculated from Eq. (29) by employing the pseudo-inverse $\mathbf{Y}_B^+$ of $\mathbf{Y}_B$ and $\mathbf{Y}_A^+$ of $\mathbf{Y}_A$, and by neglecting $\mathbf{\Sigma}_{\varepsilon B}$ and $\mathbf{\Sigma}_{\varepsilon A}$ (for small ε) to obtain

$$\begin{aligned}\mathbf{Z}_B &= \mathbf{Y}_B^+\mathbf{U}_{B1} \equiv \mathbf{V}_{B1}\mathbf{\Sigma}_B\mathbf{U}_{B1}^{\mathrm{T}}\mathbf{U}_{B1} = \mathbf{V}_{B1}\mathbf{\Sigma}_B,\\ \mathbf{Z}_A &= \mathbf{Y}_A^+\mathbf{U}_{A1} \equiv \mathbf{V}_{A1}\mathbf{\Sigma}_A\mathbf{U}_{A1}^{\mathrm{T}}\mathbf{U}_{A1} = \mathbf{V}_{A1}\mathbf{\Sigma}_A.\end{aligned} \tag{30}$$

The solution of Eq. (27) is then given by

$$\mathbf{C} = \mathbf{Y}_B\mathbf{Z}_B(\mathbf{Z}_A^{\mathrm{T}}\mathbf{Y}_A^{\mathrm{T}}\mathbf{X}_B\mathbf{Z}_B)^{-1}\mathbf{Z}_A^{\mathrm{T}}\mathbf{Y}_A^{\mathrm{T}}. \tag{31}$$

The final form of the solution using generalized minimum rank perturbation theory with the subspace selection algorithm and simultaneous damages can be written as

$$\begin{aligned}\Delta\mathbf{M} &= \mathbf{B}_M\mathbf{Z}_{BM}(\mathbf{Z}_{AM}^{\mathrm{T}}\mathbf{A}_M^{\mathrm{T}}\mathbf{V}_d\mathbf{Z}_{BM})^{-1}\mathbf{Z}_{AM}^{\mathrm{T}}\mathbf{A}_M^{\mathrm{T}},\\ \Delta\mathbf{D} &= \mathbf{B}_D\mathbf{Z}_{BD}(\mathbf{Z}_{AD}^{\mathrm{T}}\mathbf{A}_D^{\mathrm{T}}\mathbf{V}_d\mathbf{Z}_{BD})^{-1}\mathbf{Z}_{AD}^{\mathrm{T}}\mathbf{A}_D^{\mathrm{T}},\\ \Delta\mathbf{K} &= \mathbf{B}_K\mathbf{Z}_{BK}(\mathbf{Z}_{AK}^{\mathrm{T}}\mathbf{A}_K^{\mathrm{T}}\mathbf{V}_d\mathbf{Z}_{BK})^{-1}\mathbf{Z}_{AK}^{\mathrm{T}}\mathbf{A}_K^{\mathrm{T}},\end{aligned} \tag{32}$$

where matrices $\mathbf{Z}_{BM}$, $\mathbf{Z}_{BD}$, $\mathbf{Z}_{BK}$, and $\mathbf{Z}_{AM}$, $\mathbf{Z}_{AD}$, $\mathbf{Z}_{AK}$ from Eq. (32) are found for their respective $\mathbf{X}_B$, $\mathbf{Y}_B$, and $\mathbf{X}_A$, $\mathbf{Y}_A$ (used in Eqs. (24) and (25)).

The theory above has been developed for (proportionally) damped structures. This can easily be contracted for the case where the model does not include proportional damping by simply setting $\mathbf{D}$, $\Delta\mathbf{D}$, $\mathbf{B}_d$ and $\mathbf{A}_d$ to zero in the formulation. For simplicity, the systems explored in this paper include no proportional damping. Instead a more challenging form of (nonlinear) damping, caused by Coulomb friction is investigated.

2.2.5. Determination of left eigenvectors

The determination of the left eigenvectors of the system is an essential element of generalized minimum rank perturbation theory as revealed by Eq. (32). This section uses the cross-orthogonality properties of the modes to the system matrices to help extract the left eigenvectors. In previous work by the authors [21], the orthogonality properties of the eigenvectors of the system to the mass matrix were capitalized upon. For example, assuming that no damage occurs in the mass matrix (i.e. $\Delta\mathbf{M}=\mathbf{0}$), the following equation was used to determine the needed left eigenvectors

$$\mathbf{U}_d^{\mathrm{T}}\mathbf{M}\mathbf{V}_d=\mathbf{I}, \quad \text{so that} \quad \mathbf{U}_d^{\mathrm{T}}=\mathbf{V}_d^{-1}\mathbf{M}^{-1}. \tag{33}$$

For the case of damage in the mass matrix, Eq. (33) cannot be used. However, assuming that no damage occurs in the stiffness matrix (i.e. $\Delta\mathbf{K}=\mathbf{0}$), the following equation was used to determine the needed left eigenvectors:

$$\mathbf{U}_d^{\mathrm{T}}\mathbf{K}\mathbf{V}_d=\mathbf{\Lambda}_d^2, \quad \text{so that} \quad \mathbf{U}_d^{\mathrm{T}}=\mathbf{\Lambda}_d^2\mathbf{V}_d^{-1}\mathbf{K}^{-1}. \tag{34}$$

For the case of simultaneous damages in the mass, damping, and stiffness parameters, an iterative update approach can be used to determine the left eigenvectors and the damaged state of the system. This approach is referred to as the *iterative* generalized minimum rank perturbation theory method. The first step in this approach is to apply the procedure as if the mass matrix is healthy. Namely, use the orthogonality property given by Eq. (33) to determine a set of left eigenvectors. Then, use Eq. (32) to determine the $\Delta\mathbf{K}$ matrix and update the $\mathbf{K}$ matrix. The next step is to use the updated $\mathbf{K}$ matrix as if it is healthy. For example, use the orthogonality property given by Eq. (34). Then, use Eq. (32) to determine the $\Delta\mathbf{M}$ and update the $\mathbf{M}$ matrix. These two steps are then repeated with the most recently updated $\mathbf{M}$ and $\mathbf{K}$ matrices until the process converges. The authors have found that this procedure only takes a few iterations to reach convergence. The converged solution satisfies the following equation

$$\mathbf{\Gamma M}\dot{\mathbf{s}}+\mathbf{\Gamma K}\mathbf{s}=\mathbf{\Gamma}\xi,$$

where the matrices $\mathbf{\Gamma M}$ and $\mathbf{\Gamma K}$ are the converged matrices, $\mathbf{s}$ is the full (linear, augmented) state vector of the forced system $\mathbf{s}=[\dot{\mathbf{x}}\ \ \mathbf{x}\ \ \dot{\mathbf{y}}\ \ \mathbf{y}]^{\mathrm{T}}$, and ξ is the full forcing vector. The matrix $\mathbf{\Gamma}$ is a constant and unknown matrix. The matrix $\mathbf{\Gamma}$ can be determined by collecting snapshots of ξ in time. Denote ξ_i (for $i=1,\ldots,r$, with $r>n$) a set of r such snapshots obtained at r time instances. At those instances the augmented state vectors are denoted by $\mathbf{s}_i$. After convergence, the matrices $\mathbf{\Gamma M}$ and $\mathbf{\Gamma K}$ are known. Hence, a set of vectors ψ_i can be computed as

$$\psi_i=\mathbf{\Gamma M}\dot{\mathbf{s}}_i+\mathbf{\Gamma K}\mathbf{s}_i.$$

Grouping the vectors ψ_i and the snapshots ξ_i as columns (and using $\psi_i=\mathbf{\Gamma}\xi_i$), the matrix $\mathbf{\Gamma}$ can be determined as $\mathbf{\Gamma}=[\psi_1\ldots\psi_i\ldots\psi_r][\xi_1\ldots\xi_i\ldots\xi_r]^{+}$, where the superscript $+$ denotes the pseudo-inverse. Finally, the mass and stiffness matrices of the damaged augmented system can be calculated by multiplying the converged $\mathbf{\Gamma M}$ and $\mathbf{\Gamma K}$ matrices by $\mathbf{\Gamma}^{-1}$.

2.3. Multiple augmentations generalized minimum rank perturbation theory for damage detection

As an alternative to the approach presented in the previous subsection, in this subsection a damage detection methodology that uses *multiple augmentations* to determine damages in nonlinear parameters is developed for the case where only an *incomplete* set of eigenvectors is available, since in practice all modes and frequencies of the system would be very difficult to obtain accurately. This still requires all finite element model degrees of freedom to be measured. This approach is referred to as multiple augmentations generalized minimum rank perturbation theory. This section exploits the fact that multiple augmented system models can be used to follow the same nonlinear trajectory in order to determine the damage in the nonlinear parameters. The first step of the methodology is to identify the degrees of freedom where damage is located, similar to the previous subsection, by using Eqs. (10)–(13). Next, information from the damage location equations and multiple augmentations is used to detect the damage in the nonlinear parameters. Finally, minimum rank perturbation theory is used to detect damage in the linear portion of the system after the system matrices are updated and the system is augmented (once more) in a symmetric form.

Consider a system with cubic spring nonlinearities, and which, for simplicity, has no damping. Also for simplicity, assume that damage only occurs in the linear and nonlinear stiffness terms. The augmented system matrices have the following form:

$$\mathbf{M} = \begin{bmatrix} \mathbf{M}_O & \mathbf{0} \\ \mathbf{0} & \mathbf{N}_{AI} \end{bmatrix} \quad \text{and} \quad \mathbf{K} = \begin{bmatrix} \mathbf{K}_d & \mathbf{N}_{Sd} \\ \mathbf{N}_{CS} & \mathbf{N}_{AS} \end{bmatrix}, \tag{35}$$

where $\mathbf{M}$ and $\mathbf{K}$ are the augmented mass and stiffness matrices, $\mathbf{K}_d$ is the damaged linear stiffness matrix, $\mathbf{N}_{Sd}$ is the damaged matrix that contains the nonlinear parameters, and $\mathbf{M}_O$, $\mathbf{N}_{AI}$, $\mathbf{N}_{CS}$ and $\mathbf{N}_{AS}$ are as previously defined. The resulting eigenvalue problem can be written as

$$-\lambda_{ik}^2 \begin{bmatrix} \mathbf{M}_O & \mathbf{0} \\ \mathbf{0} & \mathbf{N}_{AI} \end{bmatrix} \begin{bmatrix} \mathbf{v}_{Lik} \\ \mathbf{v}_{Aik} \end{bmatrix} = \begin{bmatrix} \mathbf{K}_d & \mathbf{N}_{Sd} \\ \mathbf{N}_{CS} & \mathbf{N}_{ASi} \end{bmatrix} \begin{bmatrix} \mathbf{v}_{Lik} \\ \mathbf{v}_{Aik} \end{bmatrix}, \tag{36}$$

where λ_{ik} is the kth eigenvalue of the ith augmentation of the system, with $\mathbf{v}_{Lik}$ being the linear part (upper portion) of the corresponding eigenvector and $\mathbf{v}_{Aik}$ being the augmented part (lower portion) of the corresponding eigenvector.

The top part of Eq. (36) (corresponding to the actual linearized system equations alone) for two different augmentations i and j and eigenvectors numbered k and l gives the following equations:

$$\mathbf{K}_d \mathbf{v}_{Lik} + \mathbf{N}_{Sd} \mathbf{v}_{Aik} = -\lambda_{ik}^2 \mathbf{M}_O \mathbf{v}_{Lik}, \tag{37}$$

$$\mathbf{K}_d \mathbf{v}_{Ljl} + \mathbf{N}_{Sd} \mathbf{v}_{Ajl} = -\lambda_{jl}^2 \mathbf{M}_O \mathbf{v}_{Ljl}. \tag{38}$$

Premultiplying Eq. (37) by $\mathbf{v}_{Ljl}^{\mathrm{T}}$ and Eq. (38) by $\mathbf{v}_{Lik}^{\mathrm{T}}$ yields

$$\mathbf{v}_{Ljl}^{\mathrm{T}} \mathbf{K}_d \mathbf{v}_{Lik} + \mathbf{v}_{Ljl}^{\mathrm{T}} \mathbf{N}_{Sd} \mathbf{v}_{Aik} = -\lambda_{ik}^2 \mathbf{v}_{Ljl}^{\mathrm{T}} \mathbf{M}_O \mathbf{v}_{Lik}, \tag{39}$$

$$\mathbf{v}_{Lik}^{\mathrm{T}} \mathbf{K}_d \mathbf{v}_{Ljl} + \mathbf{v}_{Lik}^{\mathrm{T}} \mathbf{N}_{Sd} \mathbf{v}_{Ajl} = -\lambda_{jl}^2 \mathbf{v}_{Lik}^{\mathrm{T}} \mathbf{M}_O \mathbf{v}_{Ljl}. \tag{40}$$

Subtracting Eq. (40) from Eq. (39), using $\mathbf{K}_d = \mathbf{K}_d^{\mathrm{T}}$, substituting $\mathbf{N}_{Sd} = \mathbf{N}_S - \Delta\mathbf{N}$, and solving for $\Delta\mathbf{N}$ yields

$$\mathbf{v}_{Ljl}^{\mathrm{T}} \Delta\mathbf{N} \mathbf{v}_{Aik} - \mathbf{v}_{Lik}^{\mathrm{T}} \Delta\mathbf{N} \mathbf{v}_{Ajl} = \mathbf{v}_{Ljl}^{\mathrm{T}} \mathbf{N}_S \mathbf{v}_{Aik} - \mathbf{v}_{Lik}^{\mathrm{T}} \mathbf{N}_S \mathbf{v}_{Ajl} + (\lambda_{ik}^2 - \lambda_{jl}^2) \mathbf{v}_{Ljl}^{\mathrm{T}} \mathbf{M}_O \mathbf{v}_{Lik}. \tag{41}$$

The result is a scalar equation for each pair (i,j), with the unknowns in the $\Delta\mathbf{N}$ matrix, which correspond to nonlinear parameters in the degrees of freedom containing damage found from Eqs. (10) to (13). A separate equation can be written for each combination of different augmentations and eigenvectors. The equations obtained for each pair (i,j) can be combined and rearranged as to form

$$\begin{bmatrix} \rho_1^1 & \rho_2^1 & \cdots & \rho_p^1 \\ \rho_1^2 & \rho_2^2 & \cdots & \rho_p^2 \\ \vdots & \vdots & \ddots & \vdots \\ \rho_1^m & \rho_2^m & \cdots & \rho_p^m \end{bmatrix} \begin{bmatrix} \Delta_1 \\ \Delta_2 \\ \vdots \\ \Delta_p \end{bmatrix} = \begin{bmatrix} \beta_1 \\ \beta_2 \\ \vdots \\ \beta_m \end{bmatrix}, \tag{42}$$

where the constants ρ_r^s (for $r = 1,\ldots,p$, and $s = 1,\ldots,m$) come from combinations of entries from $\mathbf{v}_{Ljl}^{\mathrm{T}}$, $\mathbf{v}_{Lik}^{\mathrm{T}}$, $\mathbf{v}_{Aik}$, and $\mathbf{v}_{Ajl}$. The unknowns Δ_r come from elements of $\Delta\mathbf{N}$, and can be greater or less than zero. The constants β_s are computed directly from the right hand side of Eq. (41). For the case of zero measurement error, the number of equations m has to be at least equal to the number of unknowns p. More realistic scenarios, with measurement errors, require $m > p$, as discussed in the results (below).

After the damages in nonlinear parameters has been calculated, the system matrices can be updated. A new augmentation can then be generated so that it corresponds to a symmetric augmented system. The damage location algorithm can then be employed once more to determine where the damage in linear parameters resides, and finally minimum rank perturbation theory can be used to determine the extent of the damage in linear parameters.

2.4. Eigenvector filtering algorithms

The measurement and eigenvector/eigenvalue extraction noise which affects eigenanalyses performed experimentally can be alleviated by the following two filtering algorithms.

The first filtering algorithm exploits the fact that no damage can occur in the augmented equations of the system, and was first proposed by the authors [26]. The filtering algorithm uses the fact that no damage can occur in the augmented equations, which implies that asymmetric damage scenarios may occur. The algorithm filters all q measured eigenvectors of the system by placing them into Eq. (9). Then, for each eigenvector one enforces that no damage can occur in the elements of $\mathbf{d}_i$ corresponding to the augmented degrees of freedom. This is done by calculating new entries for the eigenvector in the augmented degrees of freedom corresponding to zero damage. This calculation is done by balancing each eigenvector component exactly with the eigenvector components that couple with it (the degrees of freedom that contain the nonlinearity). Since there should never be any damage in the augmented equations, this filtering algorithm can be applied *before* the damage location is determined.

The second filtering algorithm, which was developed by Zimmerman and Kaouk [19], is also useful in reducing the effects of noise. This filtering algorithm is used *after* the damage location is determined. It is assumed that the nonzero elements of the vector $\mathbf{d}_i$ associated with undamaged degrees of freedom are due to eigenvector errors, and can be set to zero. The result is a filtered (and augmented) damage vector $\mathbf{d}_{fi}$, which can then be used to obtain the ith filtered eigenvector $\mathbf{v}_{dfi}$ using

$$(\lambda_{di}^2\mathbf{M}+\mathbf{K})\mathbf{v}_{dfi}=\mathbf{d}_{fi}.$$

3. Results

To demonstrate the proposed method, numerical simulations on nonlinear systems of the type shown in Figs. 2–4 are performed. Matrices $\mathbf{M}_O$, $\mathbf{K}_O$, $\mathbf{N}_I$, $\mathbf{N}_S$, $\mathbf{N}_{AI}$, $\mathbf{N}_{AD}$, $\mathbf{N}_{AS}$ and $\mathbf{N}_{CS}$ were generated for each of the systems. Next, the damage detection methods discussed were implemented for each of the systems. Random measurement noise was also included to determine the sensitivity of the approaches and to estimate the effectiveness of the filtering algorithms.

3.1. Case 1: Nonlinear Kabe system

The nonlinear Kabe system shown in Fig. 2 is based on a linear Kabe system which was investigated previously by Zimmerman and Kaouk [19]. With knowledge of the linear and augmented system matrices, numerical simulations were conducted. Each mass was forced harmonically. The vector of displacements $\mathbf{x}(t)$ was calculated by standard time integration, while $\mathbf{y}(t)$ and $\mathbf{h}(t)$ were calculated based on their relation to $\mathbf{x}(t)$. The eigenvalues and eigenvectors of the augmented matrices were obtained by using the time series for $\mathbf{x}(t)$, $\mathbf{g}(t)$, $\mathbf{y}(t)$ and $\mathbf{h}(t)$. Next, the iterative generalized minimum rank perturbation theory technique was used to determine the damage location and extent by using the modal data. The iterative generalized minimum rank

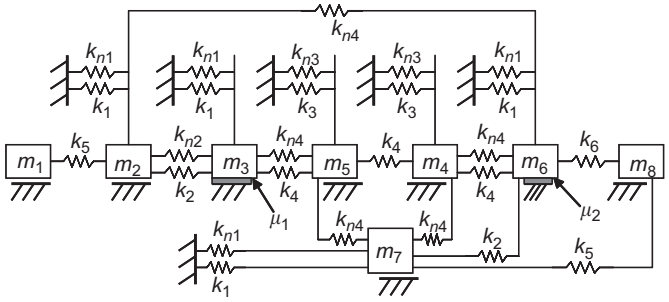

Fig. 2. A nonlinear Kabe-type problem, which also includes 12 cubic springs and Coulomb friction at two locations.

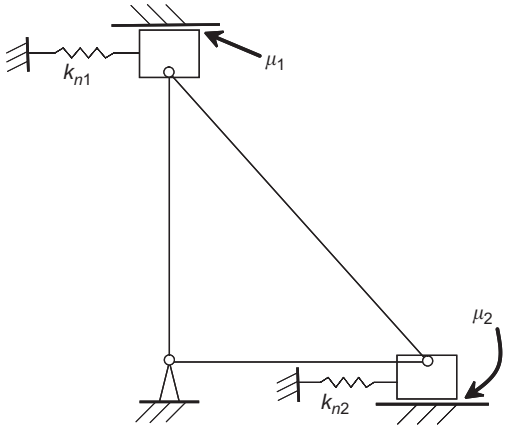

Fig. 3. Truss structure with two cubic springs and Coulomb friction at two locations.

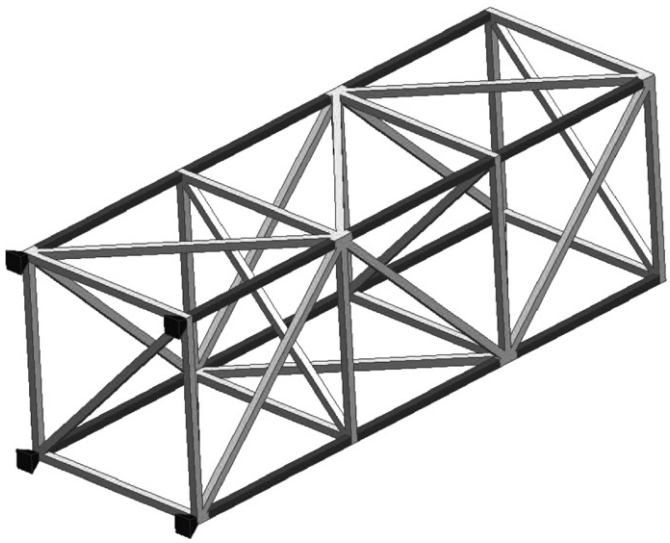

Fig. 4. Linear 3-bay structure with four cubic springs connecting joints to ground and eight cubic springs connecting joints to other joints (the dark colored elements represent nonlinear beams, while the light colored elements represent linear beams).

perturbation theory technique required the full set of the right eigenvectors to be measured to be used. Trials were conducted to show the effectiveness of calculating simultaneous damages in the mass and stiffness parameters and the effect of random noise.

To determine the effectiveness of the iterative generalized minimum rank perturbation theory method (presented in Section 2.2), a case where two linear and two nonlinear springs were damaged (in the stiffness matrix), and the Coulomb friction increased at both locations was investigated using the exact eigenvalues and right eigenvectors of the system and using noisy right eigenvectors. Fig. 5 presents element by element the values of the mass and stiffness perturbation matrices ($\Delta\mathbf{M}$ and $\Delta\mathbf{K}$) obtained using generalized minimum rank perturbation theory. The x-axes in each plot represent the index of a column vector obtained from storing the upper triangular portion of the perturbation matrix into a column vector. In order to better visualize the results every tenth index is plotted unless the absolute value of the average value of damage predicted is greater than 0.05 for (a) and 10 for (b). The y-axes in the plots represent the entries of the difference between the

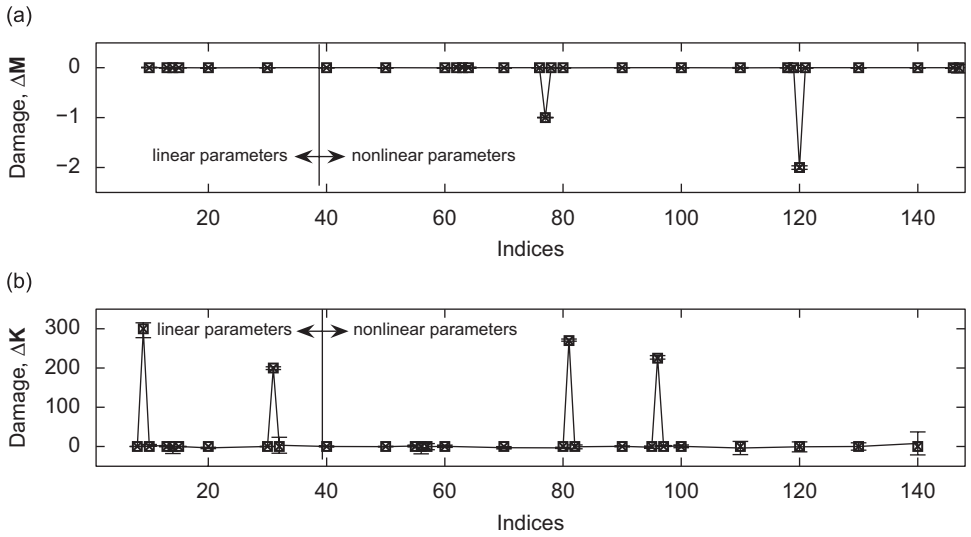

Fig. 5. Case 1: Predicted damage in the nonlinear Kabe system with damage associated with an increase in Coulomb friction (a) and a reduction of stiffness in two linear and two nonlinear springs (b) (□ exact damage; × predicted damage for no noise; – predicted damage for 5% random eigenvector noise).

original and updated matrices for (a) $\Delta\mathbf{M}$ and for (b) $\Delta\mathbf{K}$. In each plot, a line demarcates the section of linear and nonlinear parameters.

The figure illustrates how the method predicts the exact damage in both the mass and stiffness parameters when using exact eigenvalues and right eigenvectors of the system. For the case where 5% random noise was added to the right eigenvectors the average damage values for 100 separate calculations were obtained, and standard deviation error bars are plotted. The figure shows that the average value of the predicted damage is close to the exact damage. The maximum standard deviation in the damaged parameters is approximately 6% of the actual damage in that parameter.

3.2. Case 2: Nonlinear truss structure

This case explores the application of the iterative generalized minimum rank perturbation theory method (presented in Section 2.2) to a more complex structure, shown schematically in Fig. 3. The method was used to determine the damage location and extent. Trials were conducted to show the effectiveness of calculating simultaneous damages in the mass and stiffness parameters and the effect of random measurement noise.

Using the exact eigenvalues and right eigenvectors of the system, the effectiveness of the algorithm is demonstrated for a case with two damaged springs, one linear and one nonlinear (in the stiffness matrix), and an increase in Coulomb friction at one location. The results shown in Fig. 6 illustrate that the method predicts the exact damage in both the mass and stiffness parameters. Additionally, to determine the sensitivity of the iterative generalized minimum rank perturbation theory method to random measurement noise, a 10% random eigenvector and 1% random eigenvalue perturbation was added to the simulated measurements for the same case. The average damage values for 100 separate calculations were obtained and standard deviation error bars are plotted. The figure shows that the average value of the predicted damage is close to the exact damage. The maximum standard deviation in the damaged parameters is approximately 25% of the actual damage in that parameter.

3.3. Case 3: Nonlinear 3-bay structure

To demonstrate the multiple augmentations GMRPT technique (with an incomplete set of right eigenvectors, as presented in Section 2.3), a numerical investigation of a nonlinear system of the type shown

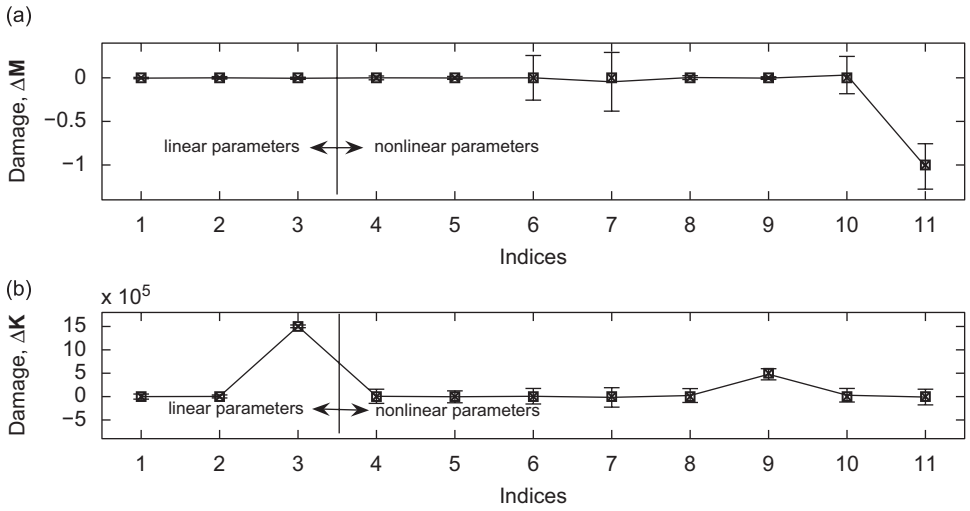

Fig. 6. Case 2: Predicted damage in the nonlinear truss system with an increase in Coulomb friction (a) and a reduction of stiffness in one linear and one nonlinear spring (b) (□ exact damage; × predicted damage for no noise; – predicted damage for 10% random eigenvector noise and 1% eigenvalue noise).

in Fig. 4 was performed. The *nonlinear* 3-bay structure is based on a linear structure. The linear 3-bay structure consists of 44 steel beams connected at 16 nodes, four of which are pinned to the ground. In addition to that, the nonlinear frame also has four cubic springs connecting nodes to ground, as well as eight cubic spring nonlinearities connecting nodes to each other and to the linear beams.

Augmented linear systems were created from the nonlinear system by obtaining the matrices $\mathbf{M}_O$, $\mathbf{K}_O$, $\mathbf{N}_I$, $\mathbf{N}_D$, $\mathbf{N}_S$, $\mathbf{N}_{AI}$, $\mathbf{N}_{AD}$, $\mathbf{N}_{AS}$ and $\mathbf{N}_{CS}$. The $\mathbf{N}_S$ matrix is composed of cubic spring stiffnesses, while $\mathbf{N}_I$ and $\mathbf{N}_D$ are zero. The matrix $\mathbf{N}_{AI}$ is a diagonal matrix containing the augmented masses. The augmented masses are chosen of the same order of magnitude as the linear masses that they are coupled to. The matrix $\mathbf{N}_{CS}$ is chosen to keep the system symmetric, i.e. the entries are the cubic spring stiffnesses. The matrix $\mathbf{N}_{AS}$ is a diagonal matrix containing augmented spring stiffnesses that were varied for different augmentations. Finally, $\mathbf{N}_{AD}$ is zero. For the 15 different augmentations that were performed for each scenario, the augmented spring stiffnesses k_a, were varied as follows:

$$\begin{aligned} k_{aji} &= i \cdot k_{nj}, \quad \text{for } i = 2, \ldots, 15, \\ k_{aj1} &= 1.5 \cdot k_{nj}, \end{aligned} \tag{43}$$

where k_{nj} is the cubic spring stiffness for the jth nonlinear degree of freedom, and k_{aji} is the corresponding augmented spring stiffness for the ith augmentation.

Augmented modal properties of each of these augmented systems were then used to determine damage location and extent. The number of modes used is restricted to the first 10 out of a total of 96. All 10 measured modes were used in the updating for each case by using the subspace selection algorithm (discussed in Section 2.2.4). Numerical simulations were performed to show the effectiveness of the method for incomplete measurements for various damage scenarios. Finally, different levels of noise were added to the eigenvectors for different damage levels to determine the sensitivity of the method to noise and to the amount of damage.

3.4. Case 3: Scenario 1: Damage in nonlinear parameters

The first scenario explored for case 3 is damage in purely nonlinear parameters. The multiple augmentations generalized minimum rank perturbation theory damage detection method (presented in Section 2.3) is applied in the following manner. First, the degrees of freedom affected by damage are isolated using Eqs. (10) and (13). Then, using the augmented modal properties from multiple augmentations, Eq. (42) is solved for the

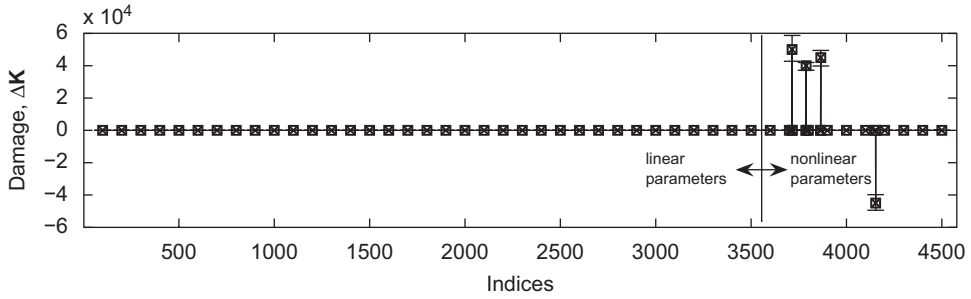

Fig. 7. Case 3: Predicted damage in a nonlinear 3-bay structure when three cubic springs are damaged (□ exact damage; × predicted damage for no noise; – predicted damage for 5% random eigenvector noise).

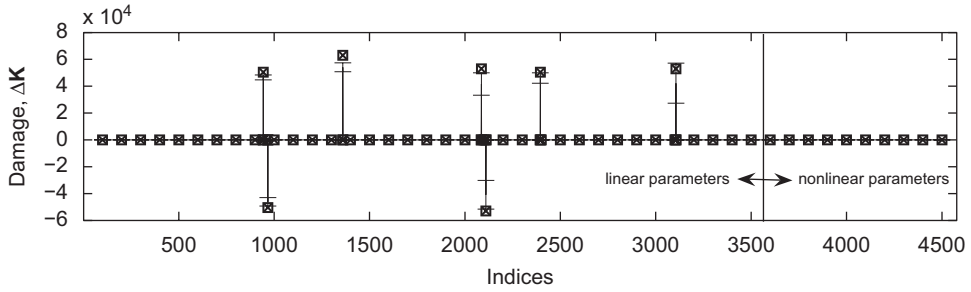

Fig. 8. Case 3: Predicted damage in a nonlinear 3-bay structure when three beams are damaged (□ exact damage; × predicted damage for no noise; – predicted damage for 5% random eigenvector noise).

damage in nonlinear parameters. Next, the damage in nonlinear parameters is incorporated, and a symmetric augmentation is produced. Finally, the degrees of freedom affected by damage are solved for again (and, as expected, no damage is found).

Results for numerical simulations where 3 cubic springs lose some of their stiffness is plotted in Fig. 7. Two of the damaged cubic springs connect nodes to ground, and one connects two nodes to each other. The percent of damages (relative to the healthy spring) in the cubic spring stiffnesses range from 40% to 50%. The plot presents element by element the values of the identified stiffness perturbation matrix $\Delta\mathbf{K}$. In order to better visualize the results every 100th index is plotted unless the absolute value of the average value of damage predicted is greater than 10. Shown are the exact value of the damage, the damage predicted using the exact eigenvectors of the system, and the damage predicted when there is 5% noise in the eigenvectors of the system. For the case of noisy data, 100 separate calculations were performed, and average and standard deviation error bars are plotted. Fig. 7 shows that, when exact eigenvectors of the system are used, damage in nonlinear parameters can be assessed exactly. Also, the average prediction is still quite accurate when there is as much as 5% random noise. The maximum standard deviation in the damaged parameters is approximately 16% of the actual damage in that parameter.

3.5. Case 3: Scenario 2: Damage in linear parameters

The second scenario examined for case 3 is damage purely in linear parameters. The methodology is carried out similarly to the scenario of damage in nonlinear parameters. However, little or no damage is predicted in the nonlinear parameters (in the presence of noise). As expected, damage is predicted when the damage location algorithm is employed a second time. Finally, generalized minimum rank perturbation theory is carried out using Eq. (32) to identify the damage in linear parameters.

Results for numerical simulations where the stiffness of three beams is reduced are plotted in Fig. 8. One of the damaged beams connects a node to ground, and two connect two nodes to each other. The percent of damages (relative to the healthy beam) in the beam stiffnesses range from 40% to 50%. The data is plotted in the same way as Fig. 7, with 100 separate calculations performed for the case of 5% noise.

The results in Fig. 8 show that, when exact eigenvectors of the system are provided, damage (in this case linear) can be assessed exactly. Also, when there is 5% random noise, the average prediction is still quite accurate, although it deviates somewhat more than the damage in nonlinear parameters (shown in Fig. 7). The maximum standard deviation in the damaged parameters is approximately 28% of the actual damage in that parameter.

3.6. Case 3: Scenario 3: Simultaneous damage in linear and nonlinear parameters

The third scenario examined for case 3 is combined damage in linear and nonlinear parameters. Similarly to the first two scenarios, after the damaged degrees of freedom are isolated using Eqs. (10) and (13), damage to the nonlinear parameters is determined using Eq. (42). Then, the system is updated (and made symmetric). Next, the damage location is identified, and finally the damage in linear parameters is determined using Eq. (32).

Results for numerical simulations where the stiffness of one beam and one cubic spring is reduced are plotted in Fig. 9. The damaged cubic spring connects two nodes to each other, and has its stiffness reduced by 45%. The damaged beam connects a node to ground, and has its stiffness reduced by 50%. The data is plotted as in Fig. 7, with 100 separate calculations performed for the case of 5% noise.

The results in Fig. 9 show that damage in both linear and nonlinear parameters can be assessed exactly when exact eigenvectors of the system are provided. Also, when there is 5% random measurement noise, the average prediction is still quite accurate. The standard deviation in the linear damaged parameter is approximately 8% of the actual damage, while the standard deviation in the nonlinear damaged parameter is approximately 6% of the actual damage.

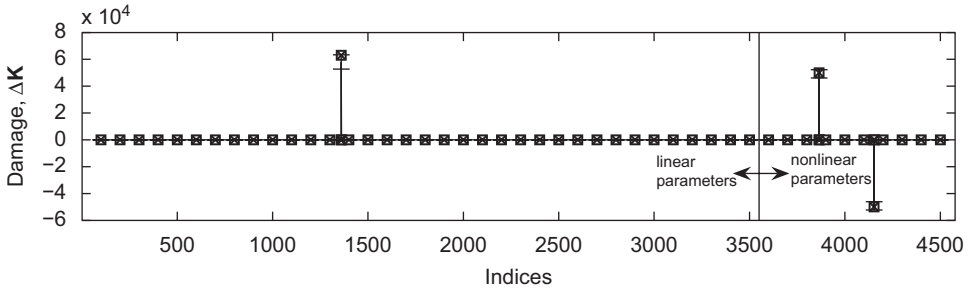

Fig. 9. Case 3: Predicted damage in a nonlinear 3-bay structure when one cubic spring and one beam are damaged (□ exact damage; × predicted damage for no noise; – predicted damage for 5% random eigenvector noise).

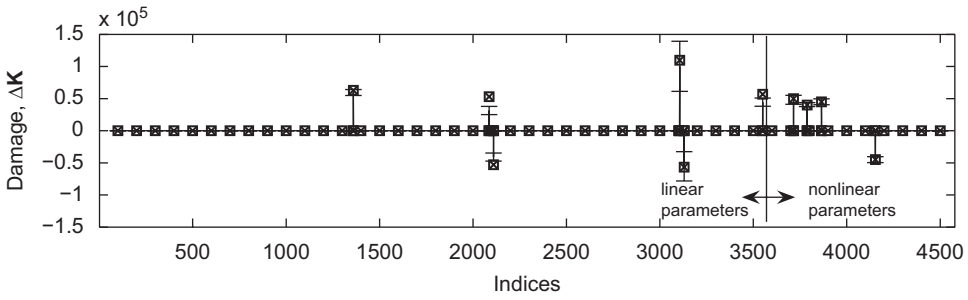

Fig. 10. Case 3: Predicted damage in a nonlinear 3-bay structure when three cubic springs and three beams are damaged (□ exact damage; × predicted damage for no noise; – predicted damage for 5% random eigenvector noise).

Results for numerical simulations where the stiffnesses of three beams and three cubic springs are reduced are plotted in Fig. 10. One of the damaged beams connects a node to ground, and two connect two nodes to each other. Two of the damaged cubic springs connect nodes to ground, and one connects two nodes to each other. The percent of damages (relative to the healthy case) ranges from 40% to 50% stiffness loss. The results are for 100 separate calculations performed for the case of 5% noise. This plot shows that, even with more complicated damage cases, the methodology works precisely when there is no noise, and it is quite accurate with as much as 5% measurement noise. The maximum standard deviation in the linear damaged parameters is approximately 35% of the actual damage, while the maximum standard deviation in the nonlinear damaged parameters is approximately 14% of the actual damage.

3.7. Case 3: Effects of noise and amount of damage

To better understand the effects of noise and of the amount of damage on the multiple augmentations generalized minimum rank perturbation theory method (presented in Section 2.3), several additional cases were examined. The results are summarized in Table 1, and consist of 10% and 50% damage to the same two elements damaged (as shown in Fig. 9) for 1%, 3%, 5%, and 10% noise. In each case, the percent error in the average predicted damage from 100 separate calculations is reported.

As expected, Table 1 shows that, in general, as the amount of noise is increased, the percent of error in the average predicted damage value is increased for both linear and nonlinear elements. Also, it is clear that the error percentage drops as the amount of damage in the elements are increased from 10% to 50%. For low noise (less than 3%) the methodology can predict damage as low as 10%. When noise is increased however, the damage location methodology fails to isolate the damaged degrees of freedom, which makes the methodology unable to predict damage. A final note is that the damage in nonlinear parameters is predicted significantly more accurately then the damage in linear parameters for the cases examined.

3.8. Effects of the eigenvector filtering algorithms on measurement noise

The effectiveness of the filtering algorithms are demonstrated in several numerical simulations. The results are summarized in Tables 2–4. Table 2 shows the results obtained by using the iterative generalized minimum rank perturbation theory method (presented in Section 2.2) for the nonlinear Kabe system (shown in Fig. 2) with 1%, 3%, and 5% random measurement noise, and for 100 separate numerical simulations. The linear spring connecting mass 2 to ground has a 10% reduction in stiffness, the nonlinear spring connecting mass 4 to ground has a 20% reduction in stiffness and the Coulomb friction between mass 6 and ground has a 35% rise in friction. Three cases were investigated, including a case where no filtering algorithms is used, a case where Zimmerman and Kaouk's filtering algorithm [19] is used alone, and a case where Zimmerman and Kaouk's filtering algorithm is used in conjunction with the new filtering algorithm proposed herein. The results in Table 2 show that the additional filtering algorithm helps reduce the effects of noise, and leads to average predicted damages closer to their exact values. In addition, since the new filtering algorithm is applied *before*

Table 1
Percent error in the average predicted damage from 100 separate calculations

Exact percent damage	Element type	Random noise %			
		1	3	5	10
		Prediction error %			
10	Linear	6.9	12.4	–	–
	Nonlinear	0.4	1.6	–	–
50	Linear	2.3	5.9	7.8	16.1
	Nonlinear	0.1	0.3	1.6	1.5

The symbol – indicates that the algorithm is unable to work because it could not identify the damaged degrees of freedom.

Table 2
Identified percent damage and the effect of the eigenvector filtering algorithms on reducing noise in the Kabe System

Filters	Exact percent damage	Random noise %		
		1	3	5
		Predicted % damage		
No filter	10	9.9	9.8	–
	20	20.0	19.8	–
	35	28.0	24.3	–
Filter 1	10	10.0	9.9	–
	20	20.0	19.8	–
	35	28.7	23.5	–
Filters 1 and 2	10	10.0	10.0	9.9
	20	20.1	20.1	20.2
	35	35.1	24.7	30.5

Filter 1 was proposed by Zimmerman and Filter 2 is the new filtering algorithm proposed herein. The symbol – indicates that the methodology was not used because the damage location could not be identified.

Table 3
Identified percent damage and the effect of the eigenvector filtering algorithms on reducing noise in the 2 degree of freedom truss system

Filters	Exact percent damage	Random noise %		
		2	5	10
		Predicted % damage		
No filter	10	10.7	–	–
	20	19.9	–	–
	30	28.0	–	–
Filter 1	10	9.8	–	–
	20	20.0	–	–
	30	30.3	–	–
Filters 1 and 2	10	10.0	9.9	10.4
	20	20.0	20.0	19.9
	30	30.0	30.3	28.3

Filter 1 was proposed by Zimmerman and Filter 2 is the new filtering algorithm proposed herein. The symbol – indicates that the methodology was not used because the damage location could not be identified.

the damage location algorithm is used, it helps the damage location algorithm as well, which allows the iterative generalized minimum rank perturbation theory method to work for larger amounts of noise.

Similar to Table 2, Table 3 also shows results obtained by using the iterative generalized minimum rank perturbation theory method, but for the nonlinear truss structure (shown in Fig. 3) with 2%, 5%, and 10% random measurement noise, and for 100 separate numerical simulations. The linear stiffness connecting mass 2 to ground has 20% damage, the nonlinear spring connecting mass 2 to ground has 10% damage, and the Coulomb friction at the second degree of freedom is increased by 30%. Each of these cases were performed for the same filtering scenarios as in Table 2. It is demonstrated that the additional filtering algorithm helps obtain a better estimate of the state of damage. Additionally, it enables the iterative generalized minimum rank perturbation theory method to work for 5% and even 10% random measurement noise.

Table 4 shows the results obtained using the multiple augmentations generalized minimum rank perturbation theory method (presented in Section 2.3) for the nonlinear 3-bay structure with 1%, 3%, and 5% random measurement noise, and for 100 separate numerical simulations. The linear beam connecting the 19th degree of freedom to ground is reduced by 10%, the nonlinear spring connecting the 13th degree of

Table 4
Identified percent damage and the effect of the eigenvector filtering algorithms on reducing noise in the 3-bay structure

Filters	Exact percent damage	Random noise %		
		1	3	5
		Predicted % damage		
No filter	10	8.6	7.9	–
	20	20.0	19.2	–
	35	35.0	34.3	–
Filter 1	10	9.3	7.8	–
	20	20.0	19.4	–
	35	35.0	34.5	–
Filters 1 and 2	10	9.2	8.3	7.8
	20	19.9	19.9	19.8
	35	34.7	34.8	33.8

Filter 1 was proposed by Zimmerman and Filter 2 is the new filtering algorithm proposed herein. The symbol – indicates that the methodology was not used because the damage location could not be identified.

freedom to ground is reduced by 35%, and the nonlinear spring connecting the 25th degree of freedom to the 49th is reduced by 20%. The same filtering cases were performed as in Table 2. The additional filtering algorithm, generally alleviates the effects of noise and allows the multiple augmentations generalized minimum rank perturbation theory method to operate well for larger amounts of random measurement noise.

4. Conclusions

In this paper, a generalized damage detection methodology which is applicable to both linear and nonlinear systems was presented. The methodology uses a specially designed augmentation to model the nonlinear system, and a generalized minimum rank perturbation theory (GMRPT) to detect damage in the augmented system. The types of nonlinearities demonstrated herein include Coulomb friction and cubic springs. An iterative GMRPT method was used to detect simultaneous damages in mass and stiffness parameters for lower-dimensional systems. Also, multiple augmentations GMRPT was used to determine damage in linear and nonlinear parameters when an incomplete set of right eigenvectors is available (and) for high-dimensional systems. Finally, two eigenvector filtering algorithms were presented that reduce the effects of random measurement noise on the accuracy of both damage detection methods. The new filtering algorithm enables these methodologies to discern the damage location when the level of noise is larger, thus allowing damage to be detected accurately when the measurement data is more corrupted by noise. The algorithms proposed have been demonstrated numerically for several different nonlinear systems. The effectiveness of the proposed methods were demonstrated, and the effects of measurement errors were presented.

Acknowledgments

The authors wish to acknowledge the National Science Foundation (CAREER program and Graduate Research Fellowship Program) and Professor Edwardo Misawa and Dr. Shih-Chi Liu (program directors) for the generous support of this work.

References

[1] Q.J. Yang, P.Q. Zhang, C.Q. Li, X.P. Wu, A system theory approach to multi-input multi-output modal parameters identification methods, *Mechanical Systems and Signal Processing* 8 (1994) 159–174.

[2] H. Vold, G. T. Rocklin, The numerical implementation of a multi-input modal estimation for mini-computers, *Proceedings of the 1st International Modal Analysis Conference*, Vol. 1, Orlando, FL, November 1982, pp. 542–548.
[3] J.N. Juang, R.S. Pappa, An eigensystem realisation algorithm for modal parameter identification and model reduction, *Journal of Guidance, Control, and Dynamics* 8 (1985) 620–627.
[4] W. Shong, P.Q. Zhang, MIMO ITD identifying technique for mini-computer, *Journal of University of Science and Technology of China* 18 (1988) 195–202.
[5] P.Q. Zhang, C.Q. Li, Q.J. Yang, Identification of structural modal parameters by ARMAV model method, *Journal of Experimental Mechanics* 4 (1989) 137–145.
[6] J. Leuridan, Some Direct Parameter Model Identification Methods Applicable for Multiple Modal Analysis, Ph.D. Thesis, University of Cincinnati, 1984.
[7] F.X. Wang, A.K. Bajaj, K. Kamiya, Nonlinear normal modes and their bifurcations for an inertially coupled nonlinear conservative system, *Nonlinear Dynamics* 42 (2005) 233–265.
[8] S.R. Ibrahim, A.A. Saafan, Correlation of analysis in modeling and structures, assessment and review, *Proceedings of the Fifth International Modal Analysis Conference*, Vol. 2, London, England, April 1987, pp. 1651–1660.
[9] W. Heylen, P. Sas, Review of model optimization techniques, *Proceedings of the Fifth International Modal Analysis Conference*, Vol. 2, London, UK, April 1987, pp. 1172–1182.
[10] A.Y.T. Leung, L.F. Chen, W.L. Wang, A linearized procedure for solving inverse sensitivity equations of non-defective systems, *Journal of Sound and Vibration* 259 (2003) 513–524.
[11] A.N. Andry, E.Y. Shapiro, J.C. Chung, Eigenstructure assignment for linear-systems, *IEEE Transactions on Aerospace and Electronic Systems* 19 (1983) 711–739.
[12] T.W. Lim, Structural damage detection using constrained eigenstructure assignment, *Journal of Guidance, Control, and Dynamics* 18 (1995) 411–418.
[13] L.J. Jiang, J. Tang, K.W. Wang, An optimal sensitivity-enhancing feedback control approach via eigenstructure assignment for structural damage identification, *ASME Journal of Vibration and Acoustics* 129 (6) (2007) 771–783.
[14] H.S. Kim, Y.S. Chun, Structural damage assessment of building structures using dynamic experimental data, *Structural Design of Tall and Special Buildings* 13 (2004) 1–8.
[15] P.L. Liu, Identification and damage detection of trusses using modal data, *Journal of Structural Engineering* 121 (1995) 599–608.
[16] M. Kaouk, D.C. Zimmerman, T.W. Simmermacher, Assessment of damage affecting all structural properties using experimental modal parameters, *ASME Journal of Vibration and Acoustics* 122 (2000) 456–463.
[17] D.C. Zimmerman, Looking into the crystal ball: the continued need for multiple viewpoints in damage detection, *Key Engineering Materials: Damage Assessment of Structures* 167–168 (1999) 76–90.
[18] D.C. Zimmerman, Model validation and verification of large and complex space structures, *Inverse Problems in Engineering* 8 (2000) 93–118.
[19] D.C. Zimmerman, M. Kaouk, Structural damage detection using minimum rank update theory, *ASME Journal of Vibration and Acoustics* 116 (1994) 222–231.
[20] D.C. Zimmerman, T. Simmermacher, Model correlation using multiple static load and vibration tests, *AIAA Journal* 33 (1995) 2182–2188.
[21] K. D'Souza, B.I. Epureanu, Damage detection in nonlinear systems using system augmentation and generalized minimum rank perturbation theory, *Smart Materials and Structures* 14 (2005) 989–1000.
[22] K. D'Souza, B.I. Epureanu, System augmentation and matrix updating for damage detection in nonlinear systems, *Proceedings of the 46th AIAA/ASME/ASCE/AHS/ASC Structures, Structural Dynamics and Materials Conference*, Vol. AIAA-2005-1831, Austin, TX, April 2005, pp. 1–9.
[23] J.S. Bay, *Fundamentals of Linear State Space Theory*, McGraw-Hill, Madison, 1999.
[24] P.E. Moraal, J.W. Grizzle, Observer design for nonlinear systems with discrete-time measurements, *IEEE Transactions on Automatic Control* 40 (1995) 395–404.
[25] J. Tsinias, Observer design for nonlinear systems, *System and Control Letters* 13 (1989) 135–142.
[26] K. D'Souza, B.I. Epureanu, Minimum rank generalized subspace updating approach for nonlinear systems, *Proceedings of the 2005 International Mechanical Engineering Congress and Exposition (IMECE)*, Vol. IMECE-2005-80135, Orlando, FL, November 2005, pp. 1–10.